Table V. Atomic Positional Parameters and Equivalent Isotropic Displacement Parameters (Å^2) and Their Estimated Standard Deviations for **2a**[a]

atom	*x*	*y*	*z*	B_{eqv}
Re(1)	0.37051 (2)	0.24484 (1)	0.23156 (2)	1.984 (3)
Cl(1)	0.3776 (1)	0.4648 (1)	0.3339 (1)	2.96 (2)
Cl(2)	0.1439 (1)	0.1668 (1)	0.3243 (2)	3.42 (3)
Cl(3)	0.3043 (1)	0.0118 (1)	0.0866 (1)	3.11 (3)
N(1)	0.2642 (4)	0.2408 (4)	0.0306 (4)	2.43 (8)
N(2)	0.5077 (4)	0.3445 (4)	−0.0091 (4)	2.55 (8)
N(3)	0.5311 (4)	0.3272 (4)	0.1158 (4)	2.22 (7)
N(4)	0.4898 (4)	0.2294 (4)	0.3516 (4)	2.40 (8)
C(1)	0.1168 (6)	0.1833 (5)	−0.0183 (6)	3.1 (1)
C(2)	0.0625 (6)	0.1794 (5)	−0.1563 (6)	3.2 (1)
C(3)	0.1634 (7)	0.2371 (5)	−0.2467 (6)	3.4 (1)
C(4)	0.3142 (6)	0.2951 (5)	−0.1967 (6)	3.1 (1)
C(5)	0.3585 (5)	0.2929 (4)	−0.0590 (5)	2.53 (9)
C(6)	0.6886 (5)	0.3817 (4)	0.1682 (5)	2.43 (9)
C(7)	0.7796 (6)	0.3524 (6)	0.0708 (7)	3.5 (1)
C(8)	0.9301 (6)	0.4064 (7)	0.1203 (8)	4.6 (1)
C(9)	0.9878 (6)	0.4877 (6)	0.2662 (8)	4.2 (1)
C(10)	0.8936 (6)	0.5160 (6)	0.3628 (7)	3.5 (1)
C(11)	0.7419 (5)	0.4618 (5)	0.3133 (6)	2.8 (1)
C(12)	0.5864 (5)	0.1849 (4)	0.4025 (5)	2.50 (9)
C(13)	0.6048 (6)	0.1958 (5)	0.5520 (6)	3.1 (1)
C(14)	0.6952 (7)	0.1420 (6)	0.5988 (8)	4.5 (1)
C(15)	0.7666 (6)	0.0805 (6)	0.4990 (8)	4.3 (1)
C(16)	0.7467 (6)	0.0695 (6)	0.3494 (8)	4.3 (1)
C(17)	0.6551 (5)	0.1215 (5)	0.3018 (6)	3.1 (1)

[a] Anisotropically refined atoms are given in the form of the equivalent isotropic displacement parameter defined as $^4/_3[a^2\beta_{11} + b^2\beta_{22} + c^2\beta_{33} + ab(\cos\gamma)\beta_{12} + ac(\cos\beta)\beta_{13} + bc(\cos\alpha)\beta_{23}]$.

dimensions. During intensity data collection, three monitor reflections were rescanned after every 97 data scans, as a check on crystal and instrumental stability. These reflections did not show any significant variation in intensity during the 50 h of X-ray exposure time.

Data reduction[23] included the application of an absorption correction[24] based on azimuthal scans of nine reflections with diffractometer angle χ near 90°.

The position of the unique rhenium atom was derived from a Patterson map, and the structure was developed and refined in a sequence of alternating difference Fourier maps and least-squares refinements. The final, convergent refinement fitted positional and anisotropic displacement parameters for 25 non-hydrogen atoms, along with an overall scale factor—226 parameters in all—to 3926 data, for a data-to-parameter ratio of 17.4. These were no significant correlation effects in the final refinements, and listings of *R* factors as functions of $|F_o|$, $(\sin\theta)/\lambda$, and data collection order showed no anomalies.

A difference map following the last refinement had five peaks with density greater than 1 e/Å^3. These were all ghosts of the rhenium atom and were considered to be caused by series-termination and absorption effects.

Important crystal data and parameters related to data collection and structure refinement are given in Table IV.

Acknowledgment. Financial support received from the Council of Scientific and Industrial Research, New Delhi, India is gratefully acknowledged. Our special thanks are due to Professor F. A. Cotton for being very helpful.

Registry No. **1a**, 2569-57-5; **1b**, 87014-42-4; **1c**, 110015-48-0; **1d**, 14458-12-9; **2a**, 110015-49-1; **2a**$^+$, 110015-53-7; **2b**, 110015-50-4; **2b**$^+$, 110015-54-8; **2c**, 110015-51-5; **2c**$^+$, 110015-55-9; **2d**, 110015-52-6; **2d**$^+$, 110015-56-0; K_2ReCl_6, 16940-97-9.

Supplementary Material Available: For **2a** listings of anisotropic thermal parameters (Table VI), bond distances (Table VII), bond angles (Table VIII), and least-squares planes and dihedral angles (Table IX) and a figure showing the electronic spectrum of **2b** in acetonitrile and the infrared spectrum of **2c** in a KBr disk (9 pages); a listing of observed and calculated structure factors (20 pages). Ordering information is given on any current masthead page.

(23) Crystallographic calculations were done by a PDP-11/60 computer (RSX-11MV4.1) with programs from the package SDP-PLUS V2.2C.
(24) North, A. C. T.; Phillips, D. C.; Mathews, F. S. *Acta Crystallogr., Sect. A: Cryst. Phys., Diffr., Theor. Gen. Crystallogr.* **1968**, *A24*, 351–359.

Contribution from the Department of Chemistry, University of Nottingham, Nottingham NG7 2RD, England, and Max-Planck-Institut für Strahlenchemie, D-4330 Mülheim a.d. Ruhr, FRG

Generation of $Re_2(CO)_9(N_2)$ from $Re_2(CO)_{10}$: Identification of Photochemical Intermediates by Matrix Isolation and Liquid-Noble-Gas Techniques

Stephen Firth,[1a] Werner E. Klotzbücher,*[1b] Martyn Poliakoff,*[1a] and James J. Turner*[1a]

Received February 2, 1987

UV photolysis of $Re_2(CO)_{10}$ in liquid xenon doped with N_2 generates $Re_2(CO)_9(N_2)$ with N_2 situated in an equatorial site. Similar results are found for $Mn_2(CO)_{10}$ and $MnRe(CO)_{10}$. The same product, *eq*-$Re_2(CO)_9(N_2)$, is obtained upon narrow-band UV photolysis (313 nm) of $Re_2(CO)_{10}$ isolated in an N_2 matrix at 20 K. The mechanism is explored by low-temperature matrix isolation studies. Short-wavelength irradiation of $Re_2(CO)_{10}$ in argon matrices yields *eq*-$Re_2(CO)_9$, which upon 546-nm irradiation isomerizes to *ax*-$Re_2(CO)_9$. When the photolysis is carried out in a N_2 matrix at 10 K, no products containing N_2 are generated, but instead the coordinatively unsaturated species $Re_2(CO)_9$ is observed. $Re_2(CO)_9$ is converted to *eq*-$Re_2(CO)_9(N_2)$ by warming the matrix to 15–20 K. Conversely, narrow-band visible photolysis (546 nm) of $Re_2(CO)_9$ at 10 K in this environment yields a second isomer of $Re_2(CO)_9(N_2)$ with N_2 occupying an axial coordination site. The relevance of these matrix results to the solution photochemistry of $Re_2(CO)_{10}$ is briefly discussed.

Introduction

There is currently considerable interest in the products and mechanisms of both the thermal and photochemical[2] reactions of dinuclear metal carbonyls. In particular, for $MM'(CO)_{10}$ species (M, M' = Mn, Re) there is now strong evidence from conventional studies,[3] from flash photolysis with both UV–visible[4-6] and IR detection,[7] and from matrix isolation studies[8,9] that two primary photochemical steps are involved:

$$MM'(CO)_{10} \xrightarrow{h\nu} M(CO)_5 + M'(CO)_5 \quad (1)$$

$$MM'(CO)_{10} \xrightarrow{h\nu} MM'(CO)_9 + CO \quad (2)$$

(1) (a) University of Nottingham. (b) Max-Planck-Institut für Strahlenchemie.
(2) Meyer, T. J.; Caspar, J. V. *Chem. Rev.* **1985**, *85*, 187.
(3) Wrighton, M. S.; Ginley, D. S. *J. Am. Chem. Soc.* **1975**, *97*, 2065.
(4) Yesaka, H.; Kobayashi, T.; Yasufuku, K.; Nagakura, S. *J. Am. Chem. Soc.* **1983**, *105*, 6249.
(5) Kobayashi, T.; Yasufuku, K.; Iwai, J.; Yesaka, H.; Noda, H.; Ohtani, H. *Coord. Chem. Rev.* **1985**, *64*, 1.
(6) Rothberg, L. J.; Cooper, N. J.; Peters, K. S.; Vaida, V. *J. Am. Chem. Soc.* **1982**, *104*, 3536.
(7) Church, S. P.; Hermann, H.; Grevels, F.-W.; Schaffner, K. *J. Chem. Soc., Chem. Commun.* **1984**, 785.
(8) Hepp, A. F.; Wrighton, M. S. *J. Am. Chem. Soc.* **1983**, *105*, 5934.
(9) Dunkin, I. R.; Härter, P.; Shields, C. S. *J. Am. Chem. Soc.* **1984**, *106*, 7248.

0020-1669/87/1326-3370$01.50/0

The relative quantum yield of steps 1 and 2 depends both on the metal and on the photolysis wavelength.[10] So far, most photochemical studies have involved reactions with phosphines, which lead to substitution of the axial CO groups. The probable mechanisms involve $MM'(CO)_9$ for the production of monosubstituted species and $M(CO)_5$ for disubstituted species.[2] However, Coville[11-13] has shown that in the thermal reactions of $MM'(CO)_{10}$ catalyzed by PdO the structures of the products are determined by a delicate balance of electronic and steric effects. Thus, in general, if electronic effects dominate, as in reactions with RNC, substitution proceeds equatorially, whereas when steric effects dominate, as with bulky phosphines, substitution proceeds axially.

Following the first synthesis of a metal dinitrogen complex in 1965, many novel N_2 species have been described,[14,15] including a number in which CO has been photochemically replaced by N_2. Since most of these compounds are unstable, much use has been made of matrix isolation[16] and other low-temperature techniques,[17] including liquefied noble gases as solvents. For example, the unstable species $Cr(CO)_5(N_2)$,[18,19] $Ni(CO)_3(N_2)$,[20,21] and $Fe(CO)(NO)_2(N_2)$[22,23] have been generated by photolysis of parent compounds either in a solid N_2 matrix at 20 K or in liquid Xe or Kr doped with N_2. Furthermore, $Cr(CO)_5(N_2)$ was one of the first molecules to be investigated by flash photolysis with IR detection.[50]

The overall process is thus characterized by photochemical CO detachment followed by N_2 replacement:

$$M(CO)_x + N_2 \xrightarrow{h\nu} M(CO)_{x-1}(N_2) + CO$$

$$M(CO)_{x-1}(N_2) + N_2 \xrightarrow{h\nu} M(CO)_{x-2}(N_2)_2 + CO$$

Using the technique of matrix isolation, it was possible to demonstrate that these reactions involve coordinatively unsaturated intermediates such as $M(CO)_{x-1}$. Unfortunately, it is one of the disadvantages of matrix isolation that no information about stability can be obtained. Furthermore, IR bands are frequently "split" by solid-state effects,[24] preventing unambiguous assignments. When N_2 complexes are generated in liquid noble gases or room-temperature solutions, such splittings are absent and the wide temperature ranges of these solvents permit studies of thermal stability, but, of course, none of the very reactive unsaturated intermediates (e.g. $Ni(CO)_3$) can be detected.

In both matrix and cryosolution experiments firm identification of the species has involved conventional IR and UV–vis spectroscopy including, where appropriate, isotopic data and force field calculations. It was thus of interest to apply these techniques to an investigation of the reaction of the dinuclear species $MM'(CO)_{10}$ with N_2, to identify the products and, if possible, to understand the mechanism of the reaction.

This paper describes experiments in which $MM'(CO)_9(N_2)$ is generated in N_2-doped liquid xenon and the surprisingly complex photochemical mechanism is unraveled by matrix isolation studies. Although the use of ^{13}CO force field calculations works well for mononuclear species,[25] such calculations are difficult for dinuclear species.[26] Fortunately a satisfactory explanation of the chemistry can be obtained without resorting to ^{13}CO data. Most of our detailed experiments have been carried out with $Re_2(CO)_{10}$, but experiments with $Mn_2(CO)_{10}$ and $MnRe(CO)_{10}$ confirm that the proposed mechanism is general.

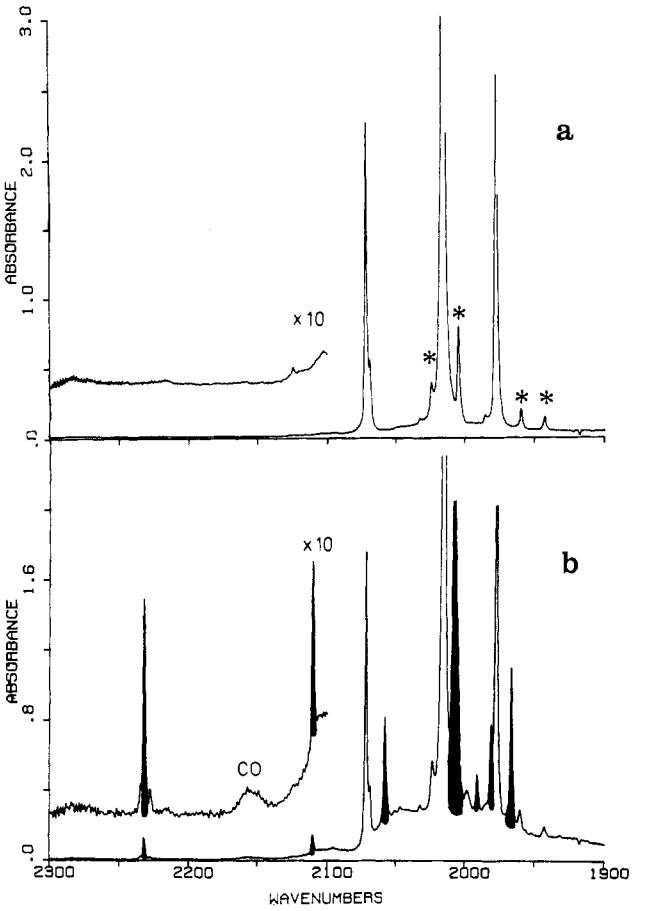

Figure 1. IR spectra illustrating UV photolysis of $Re_2(CO)_{10}$ in liquid xenon doped with N_2 at −100 °C: (a) before photolysis, bands being due to $Re_2(CO)_{10}$ and asterisks marking ^{13}CO isotopic satellites in natural abundance; (b) after brief UV photolysis (~20 s), new absorptions being colored black and associated with *eq*-$Re_2(CO)_9(N_2)$. (Note: the region 2300–2100 cm^{-1} is shown in each case on a ×10 absorbance scale.)

Experimental Section

(a) Nottingham. The detailed design of the low-temperature cryosolution cell and its specific application to organometallic photochemistry has been described previously.[21,27,28] The cell used in the experiments had an optical path length of 2.7 cm and a maximum operating pressure of 20 atm. The solution was magnetically stirred. The photolysis source was a 250-W high-pressure Hg arc ($\lambda < 280$ nm).

The matrix apparatus[29] and photolysis equipment[30] have been described previously. Matrices were prepared by slow deposition.[31] All IR spectra were obtained with a Nicolet MX-3600 FT-IR interferometer and 1280 data system. Interferograms were collected with 16K or 32K

(10) Kobayashi, T.; Ohtani, H.; Noda, H.; Teratani, S.; Yamazaki, H.; Yasufuku, K. *Organometallics* **1986**, *5*, 110.
(11) Harris, G. W.; Coville, N. J. *Organometallics* **1985**, *4*, 908.
(12) Harris, G. W.; Boeyens, J. C. A.; Coville, N. J. *J. Chem. Soc., Dalton Trans.* **1985**, 2277.
(13) Harris, G. W.; Boeyens, J. C. A.; Coville, N. J. *Organometallics* **1985**, *4*, 914.
(14) Sellmann, D. *Angew. Chem., Int. Ed. Engl.* **1974**, *13*, 639.
(15) Chatt, J.; Dilworth, J. R.; Richards, R. L. *Chem. Rev.* **1978**, *78*, 589.
(16) Hitam, R. B.; Mahmoud, K. A.; Rest, A. J. *Coord. Chem. Rev.* **1984**, *55*, 1.
(17) Turner, J. J.; Poliakoff, M.; Simpson, M. B. *J. Mol. Struct.* **1984**, *113*, 359.
(18) Burdett, J. K.; Downs, A. J.; Gaskill, G. P.; Graham, M. A.; Turner, J. J.; Turner, R. F. *Inorg. Chem.* **1978**, *17*, 523.
(19) Maier, W. B.; Poliakoff, M.; Simpson, M. B.; Turner, J. J. *J. Chem. Soc., Chem. Commun.* **1980**, 587.
(20) Rest, A. J. *J. Organomet. Chem.* **1972**, *40*, C76.
(21) Turner, J. J.; Simpson, M. B.; Poliakoff, M.; Maier, W. B. *J. Am. Chem. Soc.* **1983**, *105*, 3898.
(22) Crichton, O.; Rest, A. J.; *J. Chem. Soc., Dalton Trans.* **1977**, 656.
(23) Gadd, G. E.; Poliakoff, M.; Turner, J. J. *Inorg. Chem.* **1984**, *23*, 630.
(24) E.g.: Horton-Mastin, A.; Poliakoff, M. *Chem. Phys. Lett.* **1984**, *109*, 587.
(25) Gregory, M. F.; Poliakoff, M.; Turner, J. J. *J. Mol. Struct.* **1985**, *127*, 247.
(26) Fletcher, S. C.; Poliakoff, M.; Turner, J. J. *Inorg. Chem.* **1986**, *25*, 3597.
(27) Gadd, G. E.; Upmacis, R. K.; Poliakoff, M.; Turner, J. J. *J. Am. Chem. Soc.* **1986**, *108*, 2547.
(28) Simpson, M. B. Ph.D. Thesis, University of Nottingham, Nottingham, England, 1982.
(29) (a) Church, S. P.; Poliakoff, M.; Timney, J. A.; Turner, J. J. *Inorg. Chem.* **1983**, *22*, 3259. (b) Fletcher, S. C. Ph.D. Thesis, University of Nottingham, Nottingham, England, 1985.
(30) Baird, M. S.; Dunkin, I. R.; Hacker, N.; Poliakoff, M.; Turner, J. J. *J. Am. Chem. Soc.* **1981**, *103*, 5190.
(31) Poliakoff, M.; Turner, J. J. *J. Chem. Soc. A* **1971**, 2403.

Table I. Position (cm^{-1}) and Assignment of Observed Carbonyl Stretching Bands of $MM'(CO)_{10}$ in Liquid-Xenon Solution at −80 °C and in N_2 Matrices at 20 K

(a) $Re_2(CO)_{10}$ and $Mn_2(CO)_{10}$

$Re_2(CO)_{10}$		$Mn_2(CO)_{10}$		
Xe[a]	N_2[b]	Xe	N_2	assign (D_{4d})
2124.3	...	2113.0	...	^{13}CO
2071.9	2074.9	2046.7	2048.9	B_2
2023.6	...	...	...	^{13}CO
2014.8	2018.8	2015.9	2017.7	E_1
2004.2	2007.3	2003.7	2005.8	^{13}CO
...	...	1995.8	...	^{13}CO
1984.4	...	...	...	^{13}CO
	1981.0		1986.5	
1979.8	1978.1	1983.6	1984.0	B_2
	1975.9		1982.7	
	1973.6		1980.8	
1959.4	...	1957.2	...	^{13}CO
1942.6	...	1950.8	...	^{13}CO

(b) $MnRe(CO)_{10}$

Xe[a]	N_2[b]	assign (C_{4v})	Xe[a]	N_2[b]	assign (C_{4v})
2126.6	2129.9	A_1		1983.8	
2056.3	2058.2	A_1	1977.9	1981.2	E
...	...			1978.4	
2019.6	2022.8	E		1975.9	
1999.8	...	^{13}CO	...	...	
...	...		...	...	
1992.4	1996.1	A_1			

[a] Liquid xenon solution at −80 °C. [b] N_2 matrix at 20 K.

data points (2- or 0.7-cm^{-1} resolution) and were transformed with boxcar apodization using 32K or 256K transform points.

$Re_2(CO)_{10}$ (Aldrich Chemicals), $Mn_2(CO)_{10}$ (Strem Chemicals, Ltd.), matrix gases (Messer Griesheim), Xe and N_2 (BOC Research Grade), and $MnRe(CO)_{10}$ (a gift from Professor J. A. Connor) were all used without further purification.

(b) Mülheim. Details of the experimental equipment used in the photochemical spectroscopic studies have been described previously.[32,33] Samples were deposited from a glass capillary held at constant temperature (27 °C) by a Peltier element assembly. When not being deposited, samples were kept well below −10 °C. Evaporation temperatures for each sample were established in each experiment by first depositing onto a quartz crystal microbalance mounted in good thermal contact to the side of the target window. In general a guest:host ratio of 1:1000 was attempted.

Infrared and UV–visible spectra were taken on the same matrix within a few minutes, with results being stored for further data evaluation on a Perkin-Elmer 3600 data station. Infrared spectra were recorded on a Perkin-Elmer 580 spectrometer, with the visible radiation of the Nernst glower removed by an Oriel germanium filter. UV–visible spectra were taken on a Perkin-Elmer 320 instrument with a variable shutter in the reference beam.

Narrow-band (ca. 13 nm) UV–visible irradiation was achieved by a combination of a 900-W Hg–Xe lamp (Hanovia 977-B 0010) with a Kratos-Schoeffel GM 252-1 monochromator, while for broad-band irradiation the light of a Philips HPK 125-W Hg lamp was passed through the appropriate air-cooled Schott cutoff filters.

Results

Photochemistry of $MM'(CO)_{10}$ in Liquid Xenon Doped with N_2. Figure 1a displays the IR spectrum in the ν(C–O) region of $Re_2(CO)_{10}$ dissolved in liquid xenon doped with ~1% N_2 at −100 °C. As expected, there are three strong bands ($2b_2 + e_1$); weaker features marked with asterisks are due to complexes with ^{13}CO in natural abundance or formally forbidden bands. The band positions for $Re_2(CO)_{10}$, $Mn_2(CO)_{10}$, and $MnRe(CO)_{10}$ are listed in Table I with assignments based on previous work.[34–36] On broad-band UV photolysis of the solution the bands due to $Re_2(CO)_{10}$ decreased in intensity, molecular CO was generated, and several new bands appeared in the terminal ν(C–O) region and a single new band in the ν(N–N) region (Figure 1b and Table II). Since these new bands, marked in black, grew in and subsequently decayed together, they are assigned to a single photoproduct, E. On extended UV photolysis the bands associated with E continued to grow, but additional ν(N–N) and ν(C–O) bands appeared due to secondary photolysis products. After photolysis ceased, there was negligible change in the intensity of the E bands over a 12-h period at −100 °C; at higher temperatures much of this complex was reconverted to $Re_2(CO)_{10}$. Species E exhibits one ν(N–N) band and at least seven ν(C–O) bands with no evidence for a band due to a bridging group. The spectra are therefore consistent with photochemical substitution of CO by N_2

$$Re_2(CO)_{10} \xrightarrow[Xe(l)/N_2]{h\nu} \underset{E}{Re_2(CO)_9(N_2)} + CO$$

in which the N_2 group is in either an axial or equatorial position.

The axial and equatorial isomers of $M_2(CO)_9L$ have C_{4v} and C_s symmetry, respectively. Group theory predicts that **1** and **2**

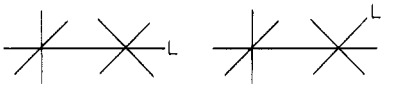

1 2

should have five and nine IR-active C–O stretching vibrations, respectively. In addition, both should have a single ν(N–N) band. Since, in liquid Xe, $Re_2(CO)_9(N_2)$ has at least seven ν(C–O) bands, the most likely structure for E is *equatorially* substituted $Re_2(CO)_9(N_2)$. Moreover, the spectrum of $Re_2(CO)_9(N_2)$ is similar to those of other equatorially substituted $M_2(CO)_9L$ species. Coville has pointed out,[11] quite correctly, that, because of unresolved bands and spectral overlap, IR spectroscopy can sometimes be misleading in attempting to distinguish between axially and equatorially substituted species. However, in this case the quality of the spectra in liquid xenon leaves little room for doubt. It is worth noting here that formation of equatorial rather than axial $Re_2(CO)_9(N_2)$ is what might have been predicted on the basis of both the electronic and steric properties of N_2.

The photolysis of $Mn_2(CO)_{10}$ and $MnRe(CO)_{10}$ in N_2-doped liquid xenon gave spectra similar to those observed for $Re_2(CO)_{10}$, showing that in each case a $MM'(CO)_9(N_2)$ species was being formed (cf. Tables I and II for the respective band positions). In the case of the mixed $MnRe(CO)_9(N_2)$ molecule there is an added complication. The N_2 could be coordinated to Re, Mn, or both. From our data it has been impossible to distinguish between these possibilities,[37] and as a result no attempt has been made to determine the stereochemistry of this molecule other than to establish that the nitrogen is equatorially bound.

Under similar conditions of temperature and photolysis the rate of production of $MM'(CO)_9(N_2)$ from $MM'(CO)_{10}$ was in the order

$$Re_2 > ReMn > Mn_2$$

This rate depends on several factors, including the UV–vis absorption spectrum of $MM'(CO)_{10}$, the output of the photolysis source, and the relative quantum yields for CO dissociation and metal–metal bond cleavage. Given that the UV–visible spectra of the compounds are similar and that the output of the lamp is constant from experiment to experiment, it is the relative quantum yields that determine the relative rates. The greater rate of production of $Re_2(CO)_9(N_2)$ is consistent with flash photolysis data, which suggest that for $Re_2(CO)_{10}$ the ratio of CO dissociation to M–M cleavage is greater than for $Mn_2(CO)_{10}$.[10]

We turn now to matrix experiments to explain the mechanism for the production of the N_2 complexes.

(32) Klotzbücher, W. E. *Cryogenics* **1983**, *23*, 554.
(33) Gerhartz, W.; Grevels, F.-W.; Klotzbücher, W. E.; Koerner von Gustorf, E. A.; Perutz, R. N. *Z. Naturforsch., B: Anorg. Chem., Org. Chem.* **1985**, *40B*, 518.
(34) Flitcroft, N.; Huggins, D. K.; Kaesz, H. D. *Inorg. Chem.* **1964**, *3*, 1123.
(35) Wozniak, W. T.; Evans, G. O.; Sheline, R. K. *J. Inorg. Nucl. Chem.* **1975**, *37*, 105.
(36) Sbrignadello, G.; Battiston, G.; Bor, G. *Inorg. Chim. Acta* **1975**, *14*, 69.
(37) Coville, N. J., private communication, 1985.

Table II. Infrared (cm^{-1}) Data of the Equatorial Dinitrogen Complexes $MM'(CO)_9(N_2)$ in Liquid Xenon Solution at −80 °C and in Solid N_2 Matrices

	$Re_2(CO)_9(N_2)$			$Mn_2(CO)_9(N_2)$		$MnRe(CO)_9(N_2)$	
	Xe[b]	N_2[a]	N_2[c]	Xe[b]	N_2[a]	Xe[b]	N_2[a]
$\nu(N_2)$	2232.3	2241.3	2241.5	2233.6	2241.2	2225.5	2229.6
$\nu(CO)$	2110.7	2113.5	2113.8	2099.1	2101.5	2113.3	2115.8
	2058.3	2060.1[d]	2061.7[d]	2037.4	2038.6	2038.4	2039.7
		2058.7[d]	2060.0[d]				
	2008.4	2013.4	2013.0	2007.6	2010.4	2011.9	2015.9
	2006.7	2007.3	2008.6	2003.7	2005.7	2008.1	2010.4
	1990.5	1991.1	...	...	1997.5	...	...
	1981.1	1982.3	1982.1	1982.2	1983.4	1975.8	1980.2
	1966.5	1966.2[d]	1967.5[d]	1969.9	...	1965.0	1964.9
		1962.4[d]	1965.4[d]				

[a] N_2 matrix at 20 K (Nottingham). [b] Liquid-xenon solution at −80 °C. [c] N_2 matrix at 10 K (Mülheim). [d] Matrix splitting.

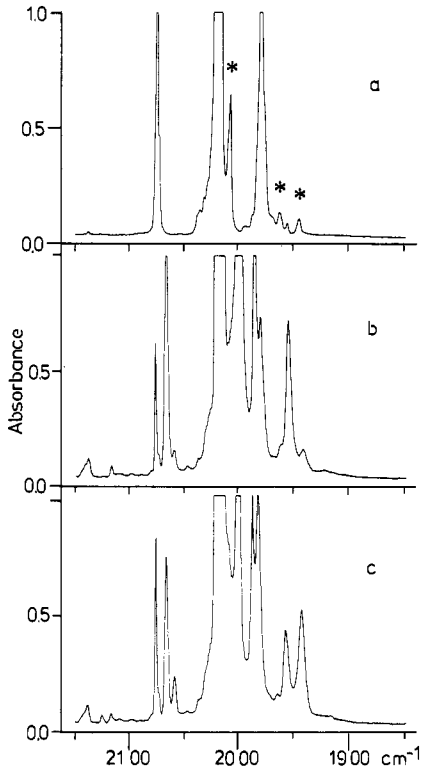

Figure 2. IR spectra illustrating the photolysis of $Re_2(CO)_{10}$ in an argon matrix at 10 K: (a) before photolysis (natural-abundance ^{13}CO satellites marked with asterisks); (b) after narrow-band UV (313 nm) photolysis, showing the bands due to unsaturated *eq*-$Re_2(CO)_9$; (c) after visible photolysis (546 nm), showing the isomerization to *ax*-$Re_2(CO)_9$ at 10 K.

Photochemistry of $Re_2(CO)_{10}$ in Argon Matrices. The infrared spectrum of $Re_2(CO)_{10}$ isolated in an argon matrix at 10 K is, apart from splittings and small frequency shifts, very similar to that in liquid xenon (Figure 2a). The characteristic carbonyl bands are located at 2076.0, 2019.7, and 1981.6 cm^{-1}. In the electronic spectrum two absorptions can be resolved at 270 and 296 nm.

Short-wavelength irradiation at 313 nm results in loss of the starting material and growth of at least five new lines in the carbonyl region at 2066, 2016, 1999, 1986, and 1956 cm^{-1}, accompanied by growth of the feature associated with "free" CO (Figure 2b). Concurrently, two new bands appear in the electronic spectrum at 390 and 530 nm (very broad).

Subsequent irradiation at 546 nm results in loss of the product on account of partial recovery of the starting material and the appearance of new absorptions at 2058, 2010, 1981, and 1942 cm^{-1} (Figure 2c). By successive irradiations at 313 and 546 nm it is possible to shift back and forth between the two photoproducts, which, as there is no evidence for a bridging carbonyl group, are probably $Re_2(CO)_9$ isomers with a vacant site in either an equatorial or axial position[38-40] (Table III).

Table III. Infrared (cm^{-1}) and UV–Vis (nm) Data of Axially and Equatorially Vacant $Re_2(CO)_9$ in Argon and Nitrogen Matrices at 10 K

eq-$Re_2(CO)_9$				*ax*-$Re_2(CO)_9$
Ar		N_2		Ar
IR	UV–vis	IR	UV–vis	IR
2066	390	2066.3	280	2058
2016	530	2016.1	390	2010
1999		1999.4	550	
1986		1984.8		1981
		1965.5		
1956		1953.4		1942

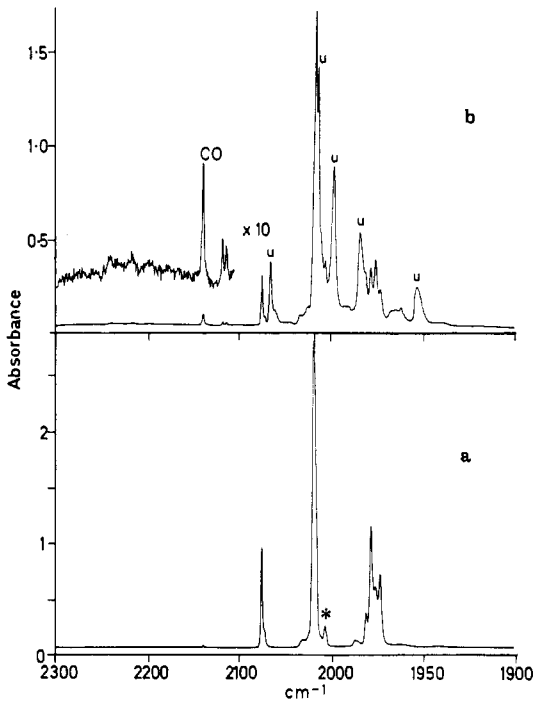

Figure 3. IR spectra illustrating the photolysis of $Re_2(CO)_{10}$ in a N_2 matrix at 10 K: (a) before photolysis (natural-abundance ^{13}CO satellites marked with asterisks); (b) after narrow-band UV (313 nm) photolysis, showing the bands due to unsaturated $Re_2(CO)_9$ (marked U). (Note: the region 2300–2100 cm^{-1} is shown on a ×10 absorbance scale).

Photochemistry of $Re_2(CO)_{10}$ in N_2 Matrices. The IR spectrum of $Re_2(CO)_{10}$ isolated in a N_2 matrix at 10 K is shown in Figure 3a; apart from matrix splittings and small frequency shifts this spectrum is very similar to that in liquid Xe (cf. part a of Table I). Narrow-band photolysis at 313 nm leads to loss of parent,

(38) Firth, S.; Hodges, P. M.; Poliakoff, M.; Turner, J. J. *Inorg. Chem.* **1986**, *25*, 4608.
(39) Shields, C. S. Ph.D. Thesis, University of Strathclyde, 1985.
(40) Klotzbücher, W. E., unpublished results.

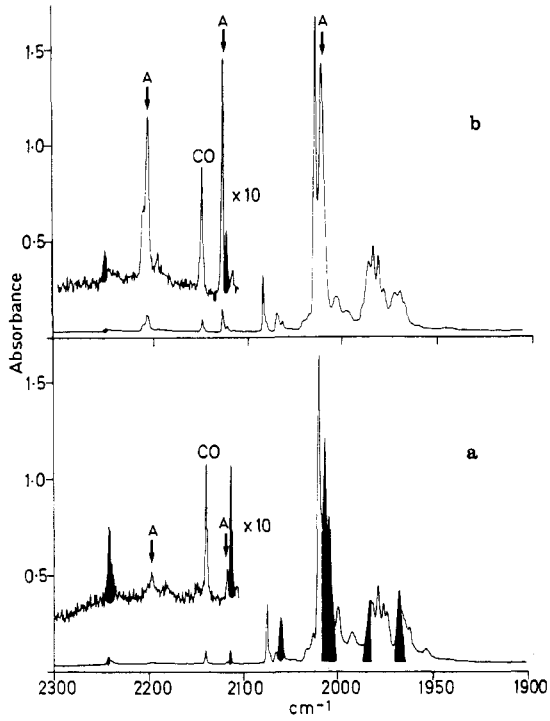

Figure 4. IR spectra illustrating the growth of dinitrogen complexes: (a) on annealing of $Re_2(CO)_9$ in a N_2 matrix (see Figure 2b) to 20 K, showing the growth of *eq*-$Re_2(CO)_9(N_2)$ (marked in black); (b) after visible photolysis (545 nm) of $Re_2(CO)_9$ in a nitrogen matrix, showing the growth of *ax*-$Re_2(CO)_9(N_2)$ (bands marked with arrows labeled A). (Note: the region 2300–2100 cm^{-1} is shown on a ×10 absorbance scale).

Table IV. Infrared (cm^{-1}) Data of the Axial Dinitrogen Complexes $MM'(CO)_9(N_2)$ in Solid N_2 Matrices

	$Re_2(CO)_9(N_2)$			
	a	*b*	$Mn_2(CO)_9(N_2)$[a]	$MnRe(CO)_9(N_2)$[a]
$\nu(N_2)$	2196.6	2197.7	2197.8	2190.2
$\nu(CO)$	2117.3	2118.8	2090.2	2109.8
		2056.4	2070.3	...
	2012.3	2013.7	2009.2	...
		1982.0		
		1968.7[c]	...	...
		1966.6[c]		

[a] N_2 matrix at 20 K (Nottingham). [b] N_2 matrix at 10 K (Mülheim). [c] Matrix-split.

the production of "free" CO, and growth of a number of absorptions in the ν(C–O) terminal region but no ν(N–N) absorption (Figure 3b). The IR and UV positions and intensities of the strong bands, labeled U in Figure 3b, are very close (allowing for a matrix shift of a few wavenumbers) to those observed (cf. Table II) when $Re_2(CO)_{10}$ is photolyzed in a pure Ar matrix.[38-40] These are assigned to $Re_2(CO)_9$ with an unbridged structure.

Annealing the matrix by warming to 15–20 K results in a decrease in the U bands and the appearance of both new ν(N–N) and ν(C–O) bands marked in black and associated with species E in Figure 4a. These bands are readily assigned to equatorial $Re_2(CO)_9(N_2)$ by comparison with our data from liquid Xe. The complex is relatively insensitive to further UV or visible photolysis in the matrix. Photolysis of $Re_2(CO)_{10}$ in an N_2 matrix at 20 K leads directly to equatorial $Re_2(CO)_9(N_2)$, presumably because $Re_2(CO)_9$ is too reactive to be observed at this higher temperature.

In contrast to the results in argon, irradiation with visible light (λ = 546 nm) of a N_2 matrix containing *eq*-$Re_2(CO)_9$ at 10 K does not yield formation of the second isomer of $Re_2(CO)_9$. Instead, the N_2-containing metal carbonyl species A is produced with a ν(N–N) absorption at a lower frequency than the ν(N–N) band of E (Figures 4b and, 5 and Table IV). Irradiation with 313-nm light destroys A and regenerates the first isomer of *eq*-$Re_2(CO)_9$, U.

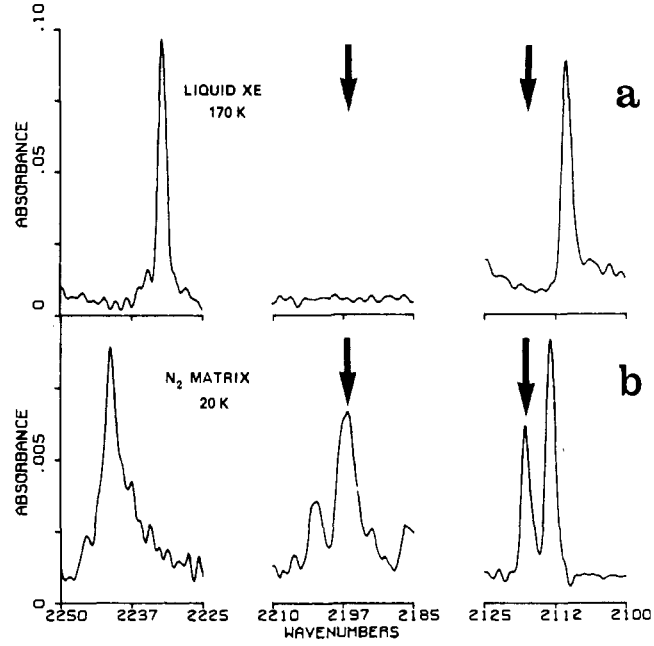

Figure 5. IR spectra of the $\nu(N_2)$ and high-frequency ν(CO) region, illustrating the differences (marked with arrows) between photoproducts produced on broad-band UV photolysis of $Re_2(CO)_{10}$ in (a) N_2-doped liquid xenon solution at −60 °C and (b) pure N_2 matrix at 20 K.

The most likely assignment for A is *axially* substituted $Re_2(CO)_9(N_2)$, but we should first consider other possibilities. Polynuclear species involving more than two Re atoms can be eliminated because formation of A is independent of the concentration of $Re_2(CO)_{10}$ in solid N_2; similarly $Re_2(CO)_8(N_2)_2$ can be eliminated because similar amounts of A were formed in both pure N_2 and N_2/Ar (1:20) matrices. In addition, formation of either $Re_2(CO)_8(N_2)_2$ or the unsaturated species $Re_2(CO)_8(N_2)$ can be eliminated because these would involve production of "free" CO and this does not occur when $Re_2(CO)_9$ is converted to A. $Re(CO)_4(N_2)$ can be excluded on account of the observation of *five* CO bands; furthermore, $Re(CO)_5$ should then also be produced (and this was not observed):

$$Re_2(CO)_9 \xrightarrow[\text{vis } h\nu]{N_2} \not\rightarrow Re(CO)_5 + Re(CO)_4(N_2)$$

The IR spectrum of $Re(CO)_5$ in matrices is known,[41,42] and there is no evidence for its formation here. Thus, the evidence suggests that A is axially substituted $Re_2(CO)_9(N_2)$.

There is an interesting isolobal analogy between $Re_2(CO)_9(N_2)$ and $CH_3Re(CO)_4(N_2)$, which also exists as the cis and trans, isomers.[43] The square-pyramidal $(OC)_5Re$ fragment is isolobal with CH_3.[44] The two isomers of $Re_2(CO)_9(N_2)$, **1** and **2**, can then be considered as cis and trans isomers of $(OC)_5Re$–$Re(CO)_4(N_2)$. *cis*-$CH_3Re(CO)_4(N_2)$ (**4**) has a ν(N–N) absorption at 2265 cm^{-1}, significantly higher in frequency than that of the trans isomer **3**, at 2204 cm^{-1}. Similarly for $(OC)_5Re$–$Re(CO)_4(N_2)$

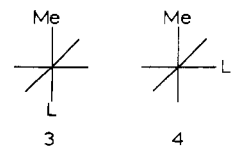

3 4

the cis isomer, E, has a higher ν(N–N) frequency than A, the trans isomer. We now show how this isolobal analogy can also lead to a better understanding of the reactions of $Re_2(CO)_9$, but first we summarize the observed photochemistry.

(41) Church, S. P.; Poliakoff, M.; Timney, J. A.; Turner, J. J. *J. Am. Chem. Soc.* **1981**, *103*, 7515.
(42) Huber, H.; Kundig, E. P.; Ozin, G. A. *J. Am. Chem. Soc.* **1974**, *96*, 5585.
(43) Horton-Mastin, A. S. L., unpublished results.
(44) Hoffman, R. *Angew. Chem., Int. Ed. Engl.* **1982**, *21*, 711.

Scheme I. Photochemistry of $Re_2(CO)_{10}$

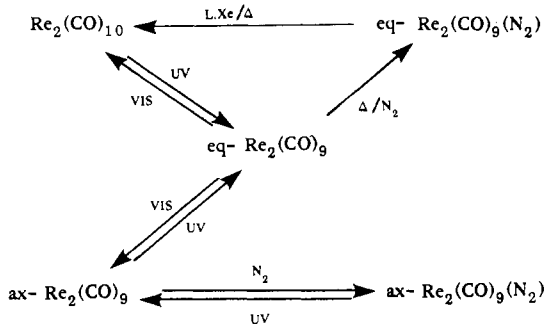

Discussion

Scheme I shows the complex photochemistry of $Re_2(CO)_{10}$, which is revealed by the matrix and liquid-xenon results. The primary photoproduct in matrices, and presumably also in liquid xenon, is the coordinatively unsaturated product $Re_2(CO)_9$ with an equatorial coordination site vacant.[38-40] In the presence of N_2, at all but the lowest temperature, *eq*-$Re_2(CO)_9$ reacts thermally with N_2 to give equatorially substituted $Re_2(CO)_9(N_2)$, E. This compound E is stable both photochemically and thermally in matrices, although in liquid xenon (at −60 °C) E decays back to parent $Re_2(CO)_{10}$ over a period of several hours.

When *eq*-$Re_2(CO)_9$ is photolyzed with visible light in argon matrices, a second unsaturated product ascribed to a second isomer of $Re_2(CO)_9$ is observed. This is reasonably assigned to a structure with a vacant axial coordination site.[38-40] Subsequent UV photolysis destroys this isomer of $Re_2(CO)_9$ and regenerates *eq*-$Re_2(CO)_9$. Visible photolysis of *eq*-$Re_2(CO)_9$ in nitrogen produces axially substituted $Re_2(CO)_9(N_2)$, A, presumably via axially vacant $Re_2(CO)_9$. The photolysis of A with UV light results in destruction of A and the re-formation of *eq*-$Re_2(CO)_9$ presumably via *ax*-$Re_2(CO)_9$.

The photochemistry of $Mn_2(CO)_{10}$ and $MnRe(CO)_{10}$ is similar to that observed for $Re_2(CO)_{10}$ with one major difference: due to the nature of the unsaturated $Mn_2(CO)_9$ and $MnRe(CO)_9$ (these species are both semibridging) very little of the axially substituted N_2 product is formed.

Photochemical Isomerization of $Re_2(CO)_9$. We have already pointed out the isolobal analogy between $Re_2(CO)_9(N_2)$ and $CH_3Re(CO)_4(N_2)$. This analogy can be extended to the coordinatively unsaturated species $Re_2(CO)_9$ and $CH_3Re(CO)_4$, both of which have two photochemically interconvertible isomers. The photoisomerization of mononuclear five-coordinate d^6 species, such as $CH_3Re(CO)_4$,[45] has been studied in considerable detail both experimentally[29,46,47] and theoretically[48,49] with the conclusion that the mechanism involves an inverse Berry pseudorotation (square pyramidal → trigonal bipyramidal → square pyramidal; see Figure 6a). Exactly the same pathway can be applied to $Re_2(CO)_9$ (Figure 6b), providing a convenient rationalization of the observed isomerization. In the mononuclear species the barrier to isomerization appears to be an intrinsic one rather than one imposed by the matrix material.[26] The same is probably true for the isomerization of $Re_2(CO)_9$.

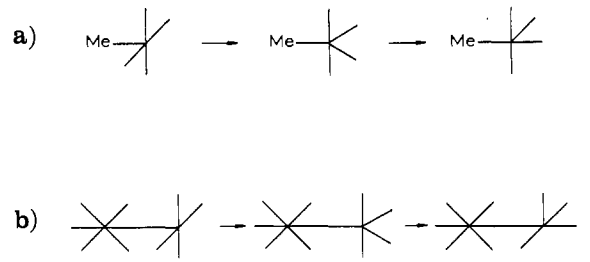

Figure 6. Comparison of the mechanisms of photoisomerization of the unsaturated species (a) $CH_3Re(CO)_4$ and (b) $Re_2(CO)_9$ by an inverse Berry pseudorotation mechanism, illustrating the application of the isolobal principle.

Mechanistic Implications of the Matrix Photochemistry. Although one must always be cautious in extrapolating from low-temperature experiments in the solid state to reactions in solution, two matrix results appear to be of potential importance in understanding the reactions of $Re_2(CO)_{10}$ in solution. These results are as follows: (i) there are two isomers of $Re_2(CO)_9$, *eq*-$Re_2(CO)_9$ and *ax*-$Re_2(CO)_9$; (ii) the activation barrier for the thermal reaction of *eq*-$Re_2(CO)_9$ with N_2 is lower than the barrier for the isomerization *eq*-$Re_2(CO)_9$ → *ax*-$Re_2(CO)_9$.

In solution as in the matrix, the primary photochemical process will presumably be generation of *eq*-$Re_2(CO)_9$, but given the intensity of conventional light sources, the lifetime of both isomers of $Re_2(CO)_9$ in solution will almost certainly be too short for significant secondary photolysis to occur. Therefore, the reactions of the intermediates in solution will be largely thermal.

The activation barrier for isomerization of $Re_2(CO)_9$ should be independent of any ligand in solution, whereas the barrier for reaction is likely to be increased by increasing steric bulk of the entering ligand. Thus, with a small entering ligand, e.g. N_2 or RNC, the rate of formation of *eq*-$Re_2(CO)_9N_2$ will be faster than isomerization to *ax*-$Re_2(CO)_9$ and hence *ax*-$Re_2(CO)_9$ will be a minor product. In contrast, for a bulky ligand isomerization will be faster and *ax*-$Re_2(CO)_9L$ will be the predominant product, exactly as observed. The matrix results therefore provide one possible rationalization of the observed solution photochemistry of $Re_2(CO)_{10}$.

Conclusions

Previous studies have shown that the photochemistry of dinuclear metal carbonyls is harder to unravel than that of mononuclear compounds.[26] In particular, matrix isolation experiments by themselves do not provide a complete picture. Here we have shown that by combining the results of matrix isolation and liquefied noble gases we have obtained a better understanding of the photosubstitution of $Re_2(CO)_{10}$ than could have been obtained from either technique alone. Our suggested mechanism for reactions in solution is now being tested by fast time-resolved IR experiments. Finally, the success of the isolobal analogy between $Re_2(CO)_9L$ and $CH_3Re(CO)_4L$ suggests that other theoretical explanations originally devised for mononuclear metal carbonyls may be extended to simple polynuclear systems.

Acknowledgment. We thank the SERC and the EEC for support. We are grateful to Dr. M. A. Healy, S. A. Jackson, Dr. R. K. Upmacis, G. Klihm, J. G. Gamble, and J. W. Whalley for their help and skilled technical assistance, to Professor J. A. Connor for a gift of $MnRe(CO)_{10}$, and to Dr. S. P. Church, Dr. F.-W. Grevels, Dr. I. R. Dunkin, Dr. C. J. Shields, and Professor J. K. Burdett for helpful discussions.

Registry No. $Re_2(CO)_{10}$, 14285-68-8; $Re_2(CO)_9(N_2)$ equatorial isomer, 109687-56-1; $Mn_2(CO)_{10}$, 10170-69-1; $MnRe(CO)_{10}$, 14693-30-2; $Re_2(CO)_9$, 109687-57-2; $Re_2(CO)_9(N_2)$ axial isomer, 109784-39-6; $Mn_2(CO)_9(N_2)$ axial isomer, 109687-58-3; $Mn_2(CO)_9(N_2)$ equatorial isomer, 109784-40-9; N_2, 7727-37-9; xenon, 7440-63-3; argon, 7440-37-1.

(45) Horton-Mastin, A.; Poliakoff, M.; Turner, J. J. *Organometallics* **1986**, *5*, 405.
(46) Burdett, J. K.; Perutz, R. N.; Poliakoff, M.; Turner, J. J. *J. Chem. Soc., Chem. Commun.* **1975**, 157.
(47) Burdett, J. K.; Grzybowski, J. M.; Perutz, R. N.; Poliakoff, M.; Turner, J. J.; Turner, R. F. *Inorg. Chem.* **1978**, *17*, 147.
(48) (a) Poliakoff, M. *Inorg. Chem.* **1976**, *15*, 2892. (b) Poliakoff, M. *Inorg. Chem.* **1976**, *15*, 2022.
(49) Burdett, J. K. *Molecular Shapes*; Wiley: New York, 1980.
(50) Church, S. P.; Grevels, F.-W.; Hermann, H.; Schaffner, K. *Inorg. Chem.* **1984**, *23*, 3830.